RSC Advances

COMMUNICATION

View Article Online
View Journal | View Issue

Cite this: *RSC Adv.*, 2016, **6**, 2028

Facet-dependent performance of BiOBr for photocatalytic reduction of Cr(VI)

Zao Fan,[a] Yubao Zhao,*[ab] Wei Zhai,[a] Liang Qiu,[a] Hui Li[a] and Michael R. Hoffmann*[b]

Received 16th September 2015
Accepted 19th December 2015

DOI: 10.1039/c5ra18768k

www.rsc.org/advances

BiOBr samples with different facets were prepared and used for photocatalytic reduction of hexavalent chromium under visible light. The results reveal that BiOBr dominated with {110} facets giving a specific rate constant 3 times as high as BiOBr with {001} facets, and its much stronger internal electric field was believed to be the main reason.

Hexavalent chromium Cr(VI) is one of the forms of chromium that poses a health risk to humans because of its high acute toxicity and carcinogenic activity. Trivalent chromium Cr(III) is much less toxic and could be easily removed from wastewater as a solid by alkalinification and precipitation. Thus, developing effective technologies capable of reducing Cr(VI) to Cr(III) is of great importance for the treatment of wastewater. Visible light driven photocatalytic reduction as a promising method to achieve this purpose has attracted extensive attention worldwide.[1]

Bismuth oxybromide BiOBr has proven itself as a kind of novel visible-light photocatalyst because the separation of photoinduced electrons and holes could be promoted by its internal static electric fields between the positive $[Bi_2O_2]$ slabs and the anionic bromine layers.[2] Li synthesized 3D flowerlike BiOBr nanostructures with an excellent removal capacity and fast adsorption rate for Cr(VI).[3] Lin obtained BiOBr nanocrystals with {001} and {010} dominant facets by hydrothermal method for degrading 2,4-dichlorophenol under UV light.[4] Zhang prepared nanosheets dominated with {102} as well as with {001} facets and compared their catalytic performance for the degradation of rhodamine B (RhB) under visible light irradiation.[5] Chen reported ultrathin BiOBr nanosheets with the {001} facet percentage of 98% showing higher photocatalytic activity than BiOBr nanoplates (63% {001}).[6] In this work, the facet-dependent photocatalytic activities of BiOBr with {001} and {110} dominant facets are systematically evaluated in the reduction of Cr(VI) ions under visible-light.

All of the chemical reagents were of analytical grade and used without further purification. BiOBr with {001} facets, named as BOB-001, was obtained by a hydrolysis process at 90 °C for 3 h using deionized water and ethanol (the volume ratio of 3 : 4) as the reaction media.[7] BiOBr dominated by the {110} facets was synthesized by treating the $Bi(NO_3)_3$–KBr–PVP–ethylene glycol system at 120 °C for 12 h, named as BOB-110.[8] The photocatalytic performance of as-prepared samples was evaluated by the reduction of Cr(VI) under visible-light irradiation at room temperature. Typically, 40 mg of BiOBr was suspended in 40 mL of 20 mg L^{-1} Cr(VI) solution, and the pH value was regulated to 3.0 by a dilute H_2SO_4 solution; after being kept in the dark for 30 min to reach the adsorption–desorption balance, the suspension with 0.5 vol% formic acid was irradiated with white 18 W-LEDs; a portion of reaction solutions, withdrawn every 10 min, was centrifuged and analyzed by 1,5-diphenylcarbazide method on a spectrophotometer (Tianjin UV-752B).

The SEM images in Fig. 1 clearly show that there exists distinct morphological feature of BiOBr samples. BOB-001 is made of numerous sheet-shaped assemblies with the size of several hundred nanometers (Fig. 1a), which is similar to the SEM observation of BiOBr dominated with {001} facets from the same preparation route: the thickness of such BiOBr lamellas was acquired as 9 nm by AFM characterization.[7] The morphology of BOB-110 is well-dispersed hierarchical microspheres with a uniform size about 1 μm, which is constructed by aggregated nanosheets (Fig. 1b).

Fig. 2 exhibits the XRD patterns of as-prepared BiOBr samples. All the patterns can be indexed to pure tetragonal phase of BiOBr (JCPDS no. 09-0393, unit cell parameters: $a = b = 3.926$ Å, $c = 8.103$ Å). The intensity ratios of {110} peak to {001} peak for BOB-110 and BOB-001 were calculated as 16.2 and 0.2, respectively. The diffraction intensity of {001} peak in BOB-001 is the strongest, confirming the high exposure of {001} facets in BOB-001. And the diffraction intensity of {110} peak for

[a]*School of Chemistry and Chemical Engineering, University of South China, Hengyang 421001, China*

[b]*Linde-Robinson Laboratory, California Institute of Technology, Pasadena, CA 91125, USA. E-mail: yubzhao@caltech.edu; mrh@caltech.edu*

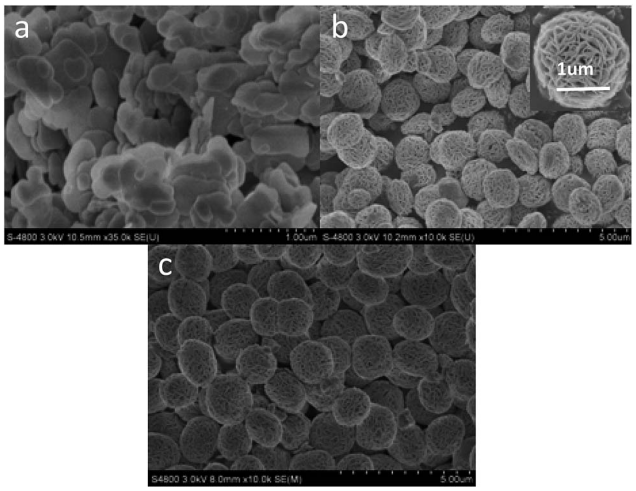

Fig. 1 SEM images of BiOBr samples (a) BOB-001, (b) BOB-110, (c) BOB-110 after five cycles.

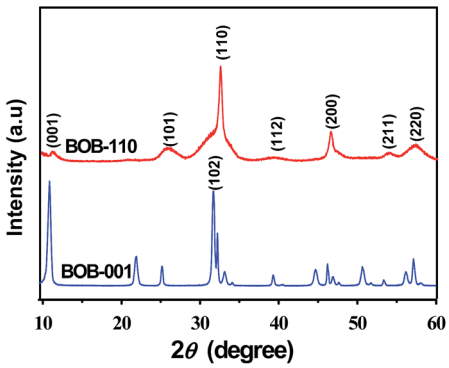

Fig. 2 XRD patterns of BiOBr.

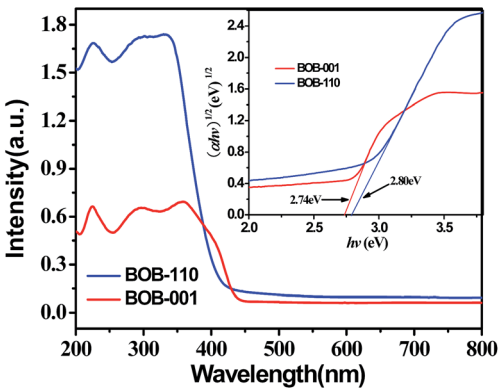

Fig. 3 UV-Visible diffuse reflectance spectra of BiOBr and the corresponding band gap energies in the insert.

sample BOB-110 is the highest among its XRD peaks, indicating that sample BOB-110 has a strong preferential tendency to develop along the [110] direction.[8]

The band structure of photocatalysts could be a critical factor to affect their catalytic performance, as it is always responsible for the efficient generation and separation of the electron–hole pairs, as well as for the response to visible light. Fig. 3 gives the UV-vis diffuse reflectance spectra (DRS) of BiOBr with different facets. All samples give the quite similar DRS features with the absorbance edge around 440 nm except that BOB-110 absorbs light more intensively than BOB-001 in UV light range. The bandgap energies of BiOB-001 and BOB-110 could be deduced as 2.74 eV and 2.80 eV, respectively, from the plots of $(\alpha h\nu)^{1/2}$ *versus* the energy of absorbed light ($h\nu$) in the insert of Fig. 3, where α is the absorbance, h the Planck constant, ν the light frequency.

It's widely accepted that the more negative the conduction band (CB) edge of photocatalysts, the higher the reduction ability of the photoexcited electrons on their CBs. The CB edges on the hydrogen scale for BiOB-001 and BOB-110 could be calculated by the empirical equation: $E_{CB}/\text{eV} = X - 0.5E_g - 4.5$, where E_{CB} is the CB edge potential; E_g the bandgap energy of semiconductors in eV; X the electronegativity of the semiconductor, which is the geometric mean of the absolute electronegativity of the constituent atoms.[9] As X is constant for a material with fixed component, it goes without saying that sample BiOBr with high E_g will have low E_{CB}. In this way, sample BOB-110 with an E_g higher than BiOB-001 by 0.06 eV, would possess an E_{CB} lower than BiOB-001 by 0.03 eV. And the low CB minimum edge would make BOB-110 give a relatively high activity for photocatalytic reduction of Cr(VI).

Fig. 4 shows the activities for Cr(VI) reduction under visible light over BOB-001 and BOB-110. BOB-110 gives much higher activity as compared with BOB-001: while the photocatalytic reaction for Cr(VI) reduction in 50 min is completed over BOB-110, almost 40% of Cr(VI) is intact for BOB-001. The pseudo-first-order reaction kinetic rate contant k of BOB-110 is 5 times as effective as that of BOB-001 (Fig. 5). As mentioned above, the E_{CB} difference of 0.03 eV seems to be a reason for their activity distinction.

Considering that the specific surface areas S_{BET} of BOB-001 and BOB-110 are 10.2 $m^2\ g^{-1}$ and 18.5 $m^2\ g^{-1}$, respectively, one might argue that the high performance of BOB-110 would probably result from its high specific surface area. In order to explore the underlying factors determining the performance of these samples besides S_{BET}, the photocatalytic activity per unit

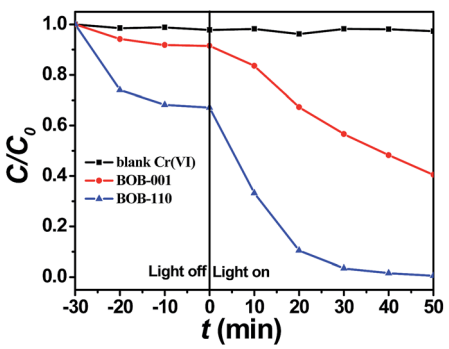

Fig. 4 Photocatalytic activity of BiOBr for Cr(VI) reduction under visible light.

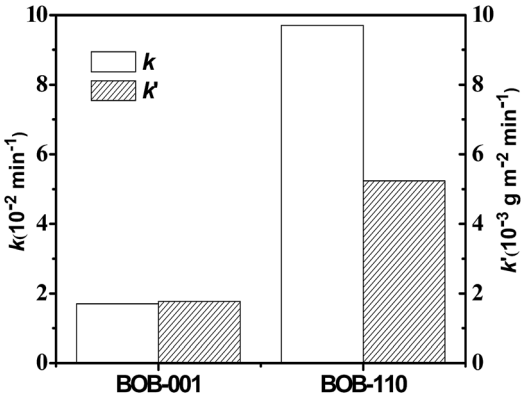

Fig. 5 The apparent first-order rate constants for catalytic reduction of Cr(VI) over BiOBr with different facets.

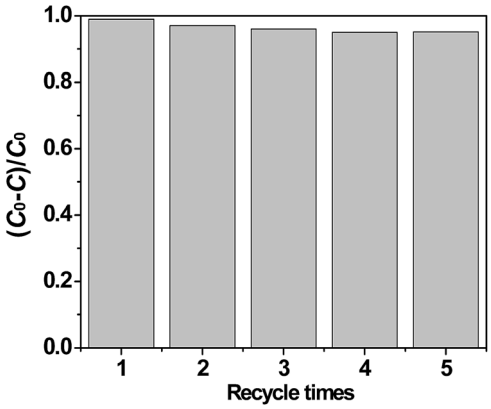

Fig. 7 Cycling runs in the photocatalytic reduction of Cr(VI) in the presence of BOB-110 under visible light.

surface area (k') would be reasonable. Kinetic results show that the specific activity k' for Cr(VI) reduction of BiOBr nanocrystals with different facets is sensitively dependent on the crystal facets: BOB-110 with preferentially exposed {110} facets is 3 times as active as BOB-001 with {001} facets (Fig. 5).

It was shown that the presence of internal electric fields (IEF) perpendicular to the positive [BiO] slabs and halogen anionic slabs in BiOX, could enable the effective separation of photoinduced electron–hole pairs along the [001] direction (Fig. 6b), and often was used as a good reason for the promising catalytic activity of BiOX with {001} facets compared to BiOX with {010} facets, which has no such IEF.[4,10,11] As to the {110} planes of BiOX, it hardly to see such explanation based on the IEF effect. The side view of atomic arrangements for {110} surface of BiOBr (Fig. 6c), clearly shows that the negatively charged [O] layers and positively charged [BiBr] layers also arranged alternatively along the [110] direction. Thus there should exist IEF for BiOBr with {110} facets, just the same case as BiOBr with {001} facets.

Based on the above results, it would be reasonable that the stronger the IEF, the more effective the separation of photogenerated carriers, and the higher the photocatalytic performance. As the distance of 1.387 Å between the [BiBr] layers and [O] layers in BiOBr with {110} facets (Fig. 6c), is obviously shorter than the distance of 2.185 Å between the [BiO] layers and [Br] layers in BiOBr with {001} facets (Fig. 6b), and the electric charge of the [O] slabs in the former is apparently higher than that of the [Br] slabs in the later, there is no doubt that sample BOB-110 dominated with {110} facets has much stronger IEF than sample BOB-001 dominated with {001} facets. As a result, the strong IEF of BiOBr dominated with {110} facets makes it a superior catalyst for photocatalytic reduction of Cr(VI).

To evaluate the stability and reusability of the BiOBr for photocatalytic reduction of Cr(VI) under visible light, BOB-110 was reused for five times. In each successive 40 min experiment, recycled sample BOB-110 was collected by centrifugation and reused under the same reaction conditions. SEM observation of such spent BOB-110 indicates that its morphology remained unchanged after recycle test (Fig. 1c). As shown in Fig. 7, no significant change in the photocatalytic activity of BOB-110 was observed after repeating 5 cycles, stating that BiOBr is stable in the present photocatalytic reduction process, just the same scenario reported for photodegradation of MO.[8]

In summary, compared to the factor of the tiny E_{CB} difference of 0.03 eV between BOB-110 and BOB-001, we believe that the distinction of IEF between them should be the main reason for the promising performance for photocatalytic reduction of Cr(VI) over BiOBr dominated with {110} facets, which has the much stronger IEF. The systematic analysis on the difference in the strength of IEF in BiOX with different facets, will be our next subject to work on.

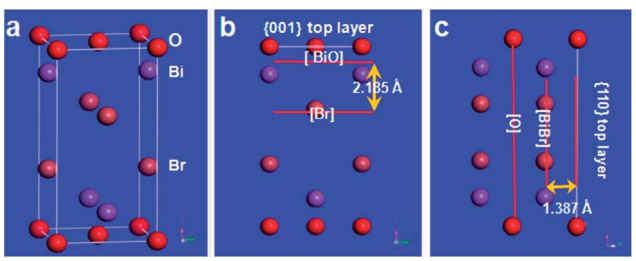

Fig. 6 The structures of (a) BiOBr crystals, side projection of (b) {001} and (c) {110} facets.

Acknowledgements

This work was supported by the Scientific Research Fund of Hunan Provincial Education Department (13B100).

Notes and references

1 G. H. Dong and L. Z. Zhang, *J. Phys. Chem. C*, 2013, **117**, 4062.
2 H. J. Zhang, L. Liu and Z. Zhou, *Phys. Chem. Chem. Phys.*, 2012, **14**, 1286.
3 G. F. Li, F. Qin, Z. Lu, H. Z. Sun and R. Chen, *Eur. J. Inorg. Chem.*, 2012, 2508.

4 W. Lin, X. Wang, Y. H. Wang, J. Y. Zhang, Z. Lin, B. T. Zhang and F. Huang, *Chem. Commun.*, 2014, DOI: 10.1039/C3CC41498A.
5 H. J. Zhang, Y. X. Yang, Z. Z. Zhou, Y. P. Zhao and L. Liu, *J. Phys. Chem. C*, 2014, **118**, 14662.
6 J. Chen, M. L. Guan, W. Z. Cai, J. J. Guo, C. Xiao and G. K. Zhang, *Phys. Chem. Chem. Phys.*, 2014, **16**, 20909.
7 D. Zhang, J. Li, Q. G. Wang and Q. S. Wu, *J. Mater. Chem. A*, 2013, **1**, 8622.
8 X. J. Shi, X. Chen, X. L. Chen, S. M. Zhou, S. Y. Lou, Y. Q. Wang and L. Yuan, *Chem. Eng. J.*, 2013, **222**, 120.
9 J. Cao, B. D. Luo, H. L. Lin, B. Y. Xu and S. F. Chen, *Appl. Catal., B*, 2012, **111**, 288.
10 J. Jiang, K. Zhao, X. Y. Xiao and L. Z. Zhang, *J. Am. Chem. Soc.*, 2012, **134**, 4473.
11 Z. K. Cui, L. W. Mi and D. W. Zeng, *J. Alloys Compd.*, 2013, **549**, 70.